# The Dynamics of Boundary Spikes for a Nonlocal Reaction-Diffusion Model

David Iron and Michael J. Ward[1]
Department of Mathematics
University of British Columbia
Vancouver, Canada

**Abstract**

An asymptotic reduction of the Gierer Meinhardt activator-inhibitor system in the limit of large inhibitor diffusivity and small activator diffusivity $\epsilon$ leads to a singularly perturbed nonlocal reaction-diffusion equation for the activator concentration. In the limit $\epsilon \to 0$, this nonlocal problem for the activator concentration has localized spike-type solutions. In this limit, we analyze the motion of a spike that is confined to the smooth boundary of a two or three-dimensional domain. By deriving asymptotic differential equations for the spike motion, it is shown that the spike moves towards a local maximum of the curvature in two dimensions and a local maximum of the mean curvature in three dimensions. The motion of a spike on a flat segment of a two-dimensional domain is also analyzed, and this motion is found to be metastable. The critical feature that allows for the slow boundary spike motion is the presence of the nonlocal term in the underlying reaction-diffusion equation.

## 1 Introduction

There has been a lot of recent interest in analyzing localized spatially inhomogeneous steady-state solutions and corresponding time-dependent solutions to systems of reaction-diffusion equations (see [14] for a mathematical survey). This work initiated with Turing in 1957 [18] who proposed that such systems could explain morphogenesis, the development of a complex organism from a single cell. Turing conjectured, through the use of a linear analysis, that a system of coupled nonlinear reaction-diffusion equations could, given appropriate conditions on the nonlinear reaction terms, result in a localized increase in the concentration of one of the substrates of the reaction. This substance, referred to as the activator, would then be responsible for the growth of cells in localized regions, leading to the development of heart tissue and other organs. Later, Gierer and Meinhardt [5], and, more recently [8] (see also the references therein), have demonstrated numerically the existence of such localized solutions in the fully nonlinear regime for the Gierer-Meinhardt model

$$A_t = \epsilon^2 \Delta A - A + \frac{A^p}{H^q}\,, \qquad \mathbf{x} \in D\,, \quad t > 0\,, \tag{1.1a}$$

$$\tau H_t = \kappa_h \Delta H - \mu H + \frac{A^m}{H^s} \qquad \mathbf{x} \in D\,, \quad t > 0\,, \tag{1.1b}$$

$$\partial_n A = 0\,, \quad \partial_n H = 0\,, \qquad \mathbf{x} \in \partial D\,. \tag{1.1c}$$

[1]This work was supported by NSERC grant 5-81541

Here $A$, $H$, $\epsilon$, $\kappa_h$, $\mu$ and $\tau$ represent the dimensionless activator concentration, inhibitor concentration, activator diffusivity, inhibitor diffusivity, inhibitor decay rate and reaction time constant. Also, $D$ is a closed bounded domain in $\mathbb{R}^N$ and $\partial_n A$ indicates the outward normal derivative. The exponents $(p, q, m, s)$ satisfy

$$p > 1, \qquad q > 0, \qquad m > 0, \qquad s \geq 0, \qquad 0 < \frac{p-1}{q} < \frac{m}{s+1}\,. \tag{1.2}$$

The shadow Gierer-Meinhardt problem is obtained by letting $\kappa_h \to \infty$ and $\tau \to 0$ in (1.1b). In this limit, (1.1) reduces to (see [10])

$$a_t = \epsilon^2 \Delta a - a + \frac{a^p}{h^q}, \qquad \boldsymbol{x} \in D\,, \quad t > 0\,, \tag{1.3a}$$

$$h = \left( \frac{\epsilon^{-N}}{\mu |D|} \int_D a^m \, d\mathbf{x} \right)^{\frac{1}{s+1}}\,, \tag{1.3b}$$

$$\partial_n a = 0\,, \qquad \boldsymbol{x} \in \partial D\,. \tag{1.3c}$$

The equilibrium solutions of (1.3) are obtained by setting $a = h^{q/(p-1)} u$, where $u$ satisfies

$$\epsilon^2 \Delta u - u + u^p = 0\,, \qquad \boldsymbol{x} \in D\,; \qquad \partial_n u = 0\,, \qquad \boldsymbol{x} \in \partial D\,. \tag{1.4}$$

The problem (1.4) admits spike-type solutions where $u$ is concentrated near some points in $D$ or on the boundary of $D$. Solutions where the spikes are located strictly inside the domain have been constructed for $\epsilon \to 0$ in many papers, including [7], [11] and [19] (see also the references theirin). In particular, the results of [7] and [11] have established the equivalence between the construction of an $M$-peak solution for (1.4) and the geometric problem of packing $M$ balls of equal radii inside the domain. All of these interior peak solutions are unstable for the parabolic problem associated with (1.4), in which a $u_t$ term is added to the right hand side of the operator in (1.4). An overview of the behavior of spike solutions for (1.4) and related equations is given in [14].

For the shadow problem (1.3), the dynamics of a one-spike solution, where the spike is in the interior of the domain, has been studied using formal asymptotic methods in [10]. For $\epsilon \to 0$ and $p < p_c(N)$, where $p_c(N)$ is the critical Sobolev exponent for dimension $N$, the analysis of [10] showed that the center $\boldsymbol{x}_0(t)$ of the spike satisfies the asymptotic differential equation

$$\mathbf{x}_0'(t) \sim \epsilon C_N \int_{\partial D} \hat{\mathbf{r}}\, r^{1-N} e^{-2r/\epsilon} (1 + \hat{\mathbf{r}} \cdot \mathbf{n}) \hat{\mathbf{r}} \cdot \mathbf{n} \, dS\,. \tag{1.5}$$

Here $\hat{\mathbf{r}} = (\mathbf{x} - \mathbf{x}_0) r^{-1}$ and $r = |\mathbf{x} - \mathbf{x}_0|$ for $\mathbf{x} \in \partial D$, $\hat{\mathbf{n}}$ is the unit outward normal to $\partial D$, and $C_N > 0$ is a constant depending only on $N$ and $p$. The ODE (1.5) shows that an interior spike will drift exponentially slowly towards the closest point on the boundary of the domain, whenever that point is uniquely defined. The nonlocal term in (1.3), which leads to a nonlocal eigenvalue problem for the linearization of (1.3) around a spike solution, is essential for ensuring the existence of this metastable behavior. Some rigorous results proving the existence of metastability for the shadow problem are given in [3] and [20].

When the spike approaches to within an $O(\epsilon)$ distance from the boundary, the analysis leading to (1.5) is no longer valid, and the spike presumably begins to merge with the boundary. In Fig. 1 we show this merging process in the simpler case of one dimension by solving (1.3) numerically with $p = 2$ and $\epsilon = .07$ using the method described in [10]. Results concerning the stability of an equilibrium boundary spike in one dimension for (1.3) are given in [22]. The merging process of a spike with the boundary should probably be similar in higher dimensions. For the equilibrium problem, the existence of boundary spike solutions to the multi-dimensional problem (1.4) has been proved in [6] and [15]. In particular, the result of [6] proved that there exists a solution to (1.4) where the spike is centered at a local maximum of the mean curvature of the boundary of a three-dimensional domain. For the parabolic problem associated with (1.4), these equilibrium solutions are all unstable (see [21]).

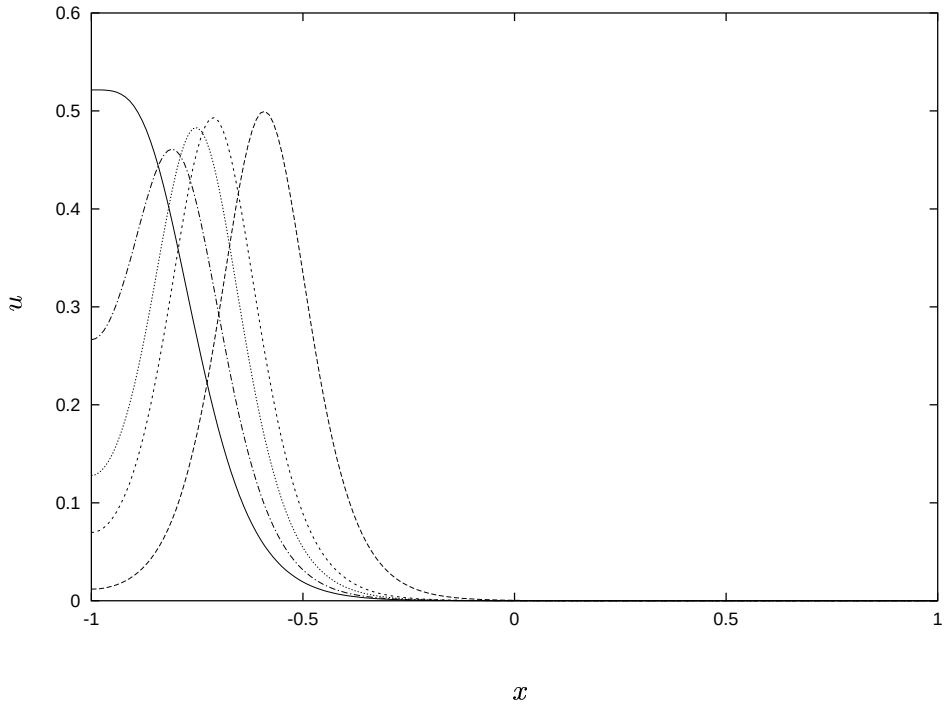


Figure 1: A plot of $u$ versus $x$ at different times showing a spike merging with the boundary in one dimension. Times from the simulation are $t = 389, 1354, 1375, 1383, 1386$ from right to left.

The goal of this paper is to analyze the motion of a spike solution to the nonlocal shadow problem (1.3), when the spike is confined to the smooth boundary of a two or three-dimensional domain. From using a formal asymptotic analysis combined with imposing appropriate solvability conditions on the linearized problem, we derive differential equations characterizing the motion of a boundary spike. This motion generically occurs on a slow

time scale of order $O(\epsilon^3)$. From this differential equation for the spike motion, we show that the spike drifts towards a local maximum of the curvature in two dimensions and a local maximum of the mean curvature in three dimensions. The nonlocal term in (1.3) is essential for ensuring the existence of this slow motion. The differential equations mentioned above predict no motion when a spike is on a segment of the boundary having constant curvature. To illustrate the spike motion in this case, we analyze the motion of a spike on a flat boundary segment of a two-dimensional domain (see Fig. 6 below for the geometrical configuration). For this case, we show that the motion is metastable and depends critically on the local behavior of the boundary near the corner points at the two ends of the flat segment.

The outline of the paper is as follows. In §2 and §3 we analyze the motion of boundary spikes for (1.3) in two and three dimensions, respectively. In §4, we examine the stability properties of the equilibrium boundary spike solutions found in §2 and §3 by using the results of [20] and [21]. Finally, in §5 we analyze the metastable behavior of a boundary spike in two dimensions that lies on a flat segment of the boundary.

## 2 Spike Motion on the Boundary in Two Dimensions

We now derive an asymptotic differential equation for the motion of a spike confined to the boundary of a two-dimensional domain. The boundary of the domain is assumed to be sufficiently smooth so that the curvature and its derivatives are continuous functions. To derive this differential equation we first transform (1.3) to a localized boundary layer coordinate system centered near the spike. The solution is then expanded in powers of $\epsilon$. A nontrivial solvability condition for the $O(\epsilon^2)$ equation in this expansion is obtained when we choose the time scale of the spike motion to be $O(\epsilon^3)$. The differential equation for the motion of the spike is obtained from this solvability condition.

We now give the details of the analysis. We first introduce a boundary layer coordinate system, where $\eta > 0$ denotes the distance from $\boldsymbol{x} \in D$ to $\partial D$ and where $s$ is arclength along $\partial D$. In terms of these coordinates, (1.3a) transforms to

$$a_t = \epsilon^2 \left( a_{\eta\eta} - \frac{\kappa}{1-\kappa\eta} a_\eta + \frac{1}{1-\kappa\eta} \partial_s \left( \frac{1}{1-\kappa\eta} a_s \right) \right) - a + a^p/h^q \,, \tag{2.1a}$$

$$a_\eta = 0 \,, \qquad \text{on} \quad \eta = 0 \,. \tag{2.1b}$$

Here $\kappa = \kappa(s)$ is the curvature of the boundary and $h = h(t)$ is given in (1.3b). Next, we introduce $u(\eta, s, t)$ by

$$a = h^\gamma u \,, \qquad \gamma = q/(p-1) \,. \tag{2.2}$$

Substituting (2.2) into (2.1) we obtain

$$\frac{\gamma u h_t}{h} + u_t = \epsilon^2 \left( u_{\eta\eta} - \frac{\kappa}{1-\kappa\eta} u_\eta + \frac{1}{1-\kappa\eta} \partial_s \left( \frac{1}{1-\kappa\eta} u_s \right) \right) - u + u^p \,, \tag{2.3a}$$

$$u_\eta = 0 \,, \qquad \text{on} \quad \eta = 0 \,. \tag{2.3b}$$

Suppose that the spike is initially located on the boundary of the domain. Then, its subsequent location is given by $s = s_0(t)$ and $\eta = 0$, where $s_0(t)$ is to be determined. Since the spike has a support of order $O(\epsilon)$ near $s_0(t)$, we introduce local variables $v$, $\hat{s}$ and $\hat{\eta}$ by

$$\hat{s} = \epsilon^{-1}\left[s - s_0(t)\right], \qquad \hat{\eta} = \epsilon^{-1}\eta, \qquad v(\hat{\eta}, \hat{s}) = u(\epsilon\hat{\eta}, s_0 + \epsilon\hat{s}, t). \tag{2.4}$$

Then, (2.3) transforms to

$$\frac{\gamma v h_t}{h} - \epsilon^{-1} s_0' v_{\hat{s}} = v_{\hat{\eta}\hat{\eta}} - \frac{\epsilon\kappa}{1-\epsilon\kappa\hat{\eta}} v_{\hat{\eta}} + \frac{1}{1-\epsilon\kappa\hat{\eta}}\partial_{\hat{s}}\left(\frac{1}{1-\epsilon\kappa\hat{\eta}} v_{\hat{s}}\right) - v + v^p, \tag{2.5a}$$

$$v_{\hat{\eta}} = 0, \qquad \text{on} \quad \hat{\eta} = 0, \tag{2.5b}$$

where $s_0' \equiv ds_0/dt$ and $\kappa = \kappa(s_0 + \epsilon\hat{s})$. Since the boundary was assumed to have a well-defined tangent plane at each point, the domain of definition for (2.5) is

$$\Omega = \{(\hat{\eta}, \hat{s}) \,|\, -\infty < \hat{s} < \infty\,, \hat{\eta} > 0\}. \tag{2.5c}$$

From differentiating the integral in (1.3b) with respect to $t$, it follows that

$$h_t = O\left(\epsilon^{-1} s_0'\right). \tag{2.6}$$

Thus, the two terms on the left hand side of (2.5a) are of the same order in $\epsilon$. However, as we show below, only one of these terms will contribute a nonzero term to a solvability condition.

The solution to (2.5a), (2.5b) is expanded as

$$v = v_0 + \epsilon v_1 + \epsilon^2 v_2 + \cdots, \tag{2.7}$$

and the curvature is expanded as

$$\kappa(s_0 + \epsilon\hat{s}) = \kappa_0 + \epsilon\hat{s}\kappa_0' + O(\epsilon^2). \tag{2.8}$$

Here we have defined $\kappa_0 \equiv \kappa(s_0)$ and $\kappa_0' \equiv \kappa'(s_0)$. Since a nontrivial solvability condition arises at order $O(\epsilon^2)$, we must choose a slow time scale $\tau$ by

$$\tau = \epsilon^3 t. \tag{2.9}$$

Substituting (2.7)–(2.9) into (2.5), and collecting powers of $\epsilon$, we obtain the following sequence of problems that are to be solved on the half-plane $\Omega$:

$$v_{0\hat{\eta}\hat{\eta}} + v_{0\hat{s}\hat{s}} + Q(v_0) = 0, \tag{2.10a}$$

$$\mathcal{L}v_1 \equiv v_{1\hat{\eta}\hat{\eta}} + v_{1\hat{s}\hat{s}} + Q'(v_0)v_1 = \kappa_0 v_{0\hat{\eta}} - 2\hat{\eta}\kappa_0 v_{0\hat{s}\hat{s}}, \tag{2.10b}$$

$$\mathcal{L}v_2 \equiv v_{2\hat{\eta}\hat{\eta}} + v_{2\hat{s}\hat{s}} + Q'(v_0)v_2 = -\dot{s}_0 v_{0\hat{s}} + \frac{\epsilon\gamma v_0 \dot{h}}{h} + F_e + F_o. \tag{2.10c}$$

Here $\dot{s}_0 \equiv ds_0/d\tau$. The boundary conditions for (2.10a)–(2.10c) are

$$v_{0\hat{\eta}} = v_{1\hat{\eta}} = v_{2\hat{\eta}} = 0\,, \qquad \text{on} \quad \hat{\eta} = 0\,. \tag{2.10d}$$

In (2.10) we have defined $Q(v_0)$ and its derivatives by

$$Q(v_0) = -v_0 + v_0^p\,, \qquad Q^{'}(v_0) = -1 + pv_0^{p-1}\,, \qquad Q^{''}(v_0) = p(p-1)v_0^{p-2}\,. \tag{2.11}$$

The terms $F_e$ and $F_o$ in (2.10c) are defined by

$$F_e = \kappa_0 v_{1\hat{\eta}} + \hat{\eta}\kappa_0^2 v_{0\hat{\eta}} - 2\hat{\eta}\kappa_0 v_{1\hat{s}\hat{s}} - \frac{Q^{''}(v_0)}{2}v_1^2 - 3\kappa_0^2\hat{\eta}^2 v_{0\hat{s}\hat{s}}\,, \tag{2.12a}$$

$$F_o = \hat{s}\kappa_0^{'} v_{0\hat{\eta}} - \hat{\eta}\kappa_0^{'} v_{0\hat{s}} - 2\hat{\eta}\hat{s}\kappa_0^{'} v_{0\hat{s}\hat{s}}\,. \tag{2.12b}$$

The leading-order problem (2.10a) has a unique positive radially symmetric solution $u_c(\rho)$ that satisfies (see [7])

$$u_c^{''} + \frac{1}{\rho}u_c^{'} + Q(u_c) = 0\,, \qquad 0 < \rho < \infty\,, \tag{2.13a}$$

$$u_c^{'}(0) = 0\,; \qquad u_c(\rho) \sim a_c \rho^{-1/2} e^{-\rho}\,, \qquad \text{as} \quad \rho \to \infty\,. \tag{2.13b}$$

Here $a_c$ is some positive constant and $\rho \equiv \left(\hat{\eta}^2 + \hat{s}^2\right)^{1/2}$. Thus, we take

$$v_0(\hat{\eta}, \hat{s}) = u_c\left[(\hat{\eta}^2 + \hat{s}^2)^{1/2}\right]\,, \tag{2.14}$$

which also satisfies the boundary condition in (2.10d). To obtain our solvability condition, we notice that the tangential derivative $v_{0\hat{s}}$ satisfies $\mathcal{L}v_{0\hat{s}} = 0$ and the boundary condition (2.10d). Hence, upon defining the inner product $(f, g) \equiv \int_\Omega fg\, d\Omega$, we must have that the right hand sides of (2.10b) and (2.10c) are orthogonal to $v_{0\hat{s}}$ with respect to this inner product. An important observation is that $v_{0\hat{s}}$ is an odd function of $\hat{s}$.

This solvability condition for (2.10b) yields,

$$\kappa_0\left(v_{0\hat{\eta}}, v_{0\hat{s}}\right) - 2\kappa_0\left(\hat{\eta}v_{0\hat{s}\hat{s}}, v_{0\hat{s}}\right) = 0\,. \tag{2.15}$$

Since $v_{0\hat{\eta}}$ and $v_{0\hat{s}\hat{s}}$ are even functions of $\hat{s}$, the integrands associated with the inner products in (2.15) are odd, and hence the left hand side of (2.15) vanishes identically. Then, we can solve (2.10b) for $v_1$ and obtain that $v_1$ is even in $\hat{s}$. Next, upon applying the solvability condition to (2.10c), we obtain

$$\dot{s}_0\left(v_{0\hat{s}}, v_{0\hat{s}}\right) = \left(F_o, v_{0\hat{s}}\right) + \left(F_e, v_{0\hat{s}}\right) + \frac{\epsilon\gamma\dot{h}}{h}\left(v_0, v_{0\hat{s}}\right)\,. \tag{2.16}$$

The significance of the decomposition in (2.10c) is that $F_e$ is even in $\hat{s}$, whereas $F_o$ is odd in $\hat{s}$. Hence, the last two terms on the right hand side of (2.16) are zero. Next, substituting (2.12b) into (2.16), we get

$$\dot{s}_0\left(v_{0\hat{s}}, v_{0\hat{s}}\right) = \kappa_0^{'}\left(\hat{s}v_{0\hat{\eta}}, v_{0\hat{s}}\right) - \kappa_0^{'}\left(\hat{\eta}v_{0\hat{s}}, v_{0\hat{s}}\right) - 2\kappa_0^{'}\left(\hat{\eta}\hat{s}v_{0\hat{s}\hat{s}}, v_{0\hat{s}}\right)\,. \tag{2.17}$$

Finally, the inner products in (2.17) are evaluated exactly using polar coordinates to get

$$(\hat{s}v_{0\hat{\eta}}, v_{0\hat{s}}) = (\hat{\eta}v_{0\hat{s}}, v_{0\hat{s}}) = \frac{2}{3}\int_0^\infty \rho^2 \left[u_c'(\rho)\right]^2 d\rho\,, \tag{2.18a}$$

$$(v_{0\hat{s}}, v_{0\hat{s}}) = \frac{\pi}{2}\int_0^\infty \rho \left[u_c'(\rho)\right]^2 d\rho\,, \tag{2.18b}$$

$$2\,(\hat{\eta}\hat{s}v_{0\hat{s}\hat{s}}, v_{0\hat{s}}) = -\frac{2}{3}\int_0^\infty \rho^2 \left[u_c'(\rho)\right]^2 d\rho\,. \tag{2.18c}$$

Substituting (2.18) into (2.17) we obtain the following main result:

**Proposition 2.1**: *For $\epsilon \to 0$, the motion of a spike confined to the smooth boundary of a two-dimensional domain is described by*

$$a \sim h^\gamma u_c\left(\epsilon^{-1}\left[(s - s_0(t))^2 + \eta^2\right]^{1/2}\right) + O(\epsilon)\,, \tag{2.19a}$$

$$s_0'(t) \sim \frac{4b}{3\pi}\epsilon^3 \kappa'(s_0)\,, \tag{2.19b}$$

*where $\gamma = q/(p-1)$ and $b > 0$ is defined by*

$$b \equiv \frac{\int_0^\infty \rho^2 \left[u_c'(\rho)\right]^2 d\rho}{\int_0^\infty \rho \left[u_c'(\rho)\right]^2 d\rho}\,. \tag{2.19c}$$

*Here $u_c(\rho)$ is the positive solution to (2.13) and $\kappa$ is the curvature of the boundary, with $\kappa > 0$ for a circle.*

From (2.19b), we observe that the spike will travel on the boundary in the direction of increasing curvature until a local maximum of the curvature is reached. The stable steady-states of (2.19b) are at the local maxima of the curvature. A similar differential equation has been derived in [1] for small bubble solutions of the constrained Allen-Cahn equation.

## 2.1 A Few Explicit Examples

We now illustrate (2.19b) in a convex domain. Let the origin be contained in $D$ and let $(x_1, x_2)$ be a point on $\partial D$. Let $\zeta$ denote the perpendicular distance from the origin to the tangent line to $\partial D$ that passes through $(x_1, x_2)$. Let $\theta$ denote the angle between this perpendicular line and the positive $x_1$ axis. Then, when $\theta$ ranges over $0 \le \theta \le 2\pi$, we sweep out a closed domain $D$ whose boundary is given parametrically by (see [9])

$$x_1(\theta) = \zeta(\theta)\cos(\theta) - \zeta'(\theta)\sin(\theta)\,, \qquad x_2(\theta) = \zeta(\theta)\sin(\theta) + \zeta'(\theta)\cos(\theta)\,. \tag{2.20}$$

Here $\zeta(\theta)$ is $2\pi$ periodic.

Next, we transform the ODE (2.19b), written in terms of arclength, to one involving $\theta$. Let $s = f(\theta)$ be the mapping between $\theta$ and the arclength $s$. Then, $f'(\theta)$ and the curvature of the boundary $\kappa(\theta)$ are given by

$$f'(\theta) = \zeta(\theta) + \zeta''(\theta)\,, \qquad \kappa(\theta) = \left[\zeta(\theta) + \zeta''(\theta)\right]^{-1}\,. \tag{2.21}$$

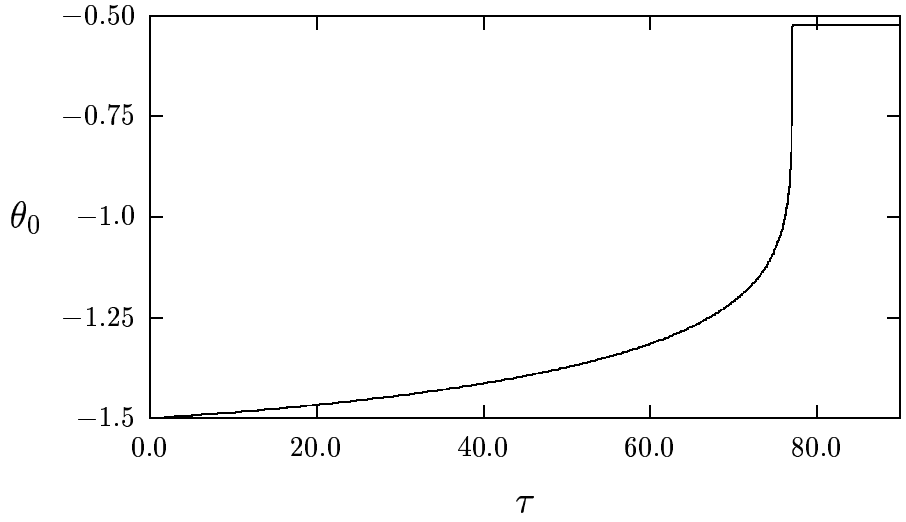


Figure 3: For Example 1 we plot the solution $\theta_0$ versus $\tau$ to (2.22) showing the behavior towards a local maximum of the curvature.

Hence, (2.19b) transforms to

$$\theta_0'(\tau) \sim -\frac{4b}{3\pi} \frac{\left[\zeta'(\theta_0) + \zeta'''(\theta_0)\right]}{\left[\zeta(\theta_0) + \zeta''(\theta_0)\right]^4}. \tag{2.22}$$

Here $\theta_0(\tau)$ is the value of $\theta$ at the center of the spike, and $\tau = \epsilon^3 t$ is the slow time variable.

Using the boundary value problem solver COLSYS [2] we can solve (2.13) numerically to determine the constant $b$ in (2.19b). In the examples below we took $p = 2$. For this value, we compute that

$$\int_0^\infty \rho^2 \left[u_c'(\rho)\right]^2 d\rho = 4.23\,, \qquad \int_0^\infty \rho \left[u_c'(\rho)\right]^2 d\rho = 2.47\,. \tag{2.23}$$

Hence, when $p = 2$, we get $b = 1.71$. In the examples below, solutions to (2.22) were computed using the Sandia ODE solver [17].

**Example 1:** Let $\zeta(\theta) = 3 + 1.2\sin^3(\theta)$, and take the initial condition for (2.22) as $\theta_0(0) = -1.5$, for which $x_1 = 0.339$ and $x_2 = -1.790$ at $\tau = 0$. The curvature has three local maxima for this domain. In Fig. 2 we plot the domain bounded by $\zeta(\theta)$ and show snapshots of the motion of the center of the spike (labeled by the starred points) towards the nearby local maximum of the curvature. In Fig. 3 we plot the numerical solution to (2.22) with $\theta_0(0) = -1.5$. For this initial value and with $\epsilon = 0.1$, this figure shows that it takes a time $t = \tau/\epsilon^3 \approx 77500.0$ to reach the steady-state value.

**Example 2:** Let $\zeta(\theta) = 3 + \cos(5\theta)/10$, and take $\theta_0(0) = 0.6$, for which $x_1 = 2.430$ and $x_2 = 1.567$ at $\tau = 0$. For this case, the ODE (2.22) becomes

$$\theta_0' = -\frac{4b}{3\pi}\left(\frac{12\sin(5\theta_0)}{\left[3 - 2.4\cos(5\theta_0)\right]^4}\right). \tag{2.24}$$

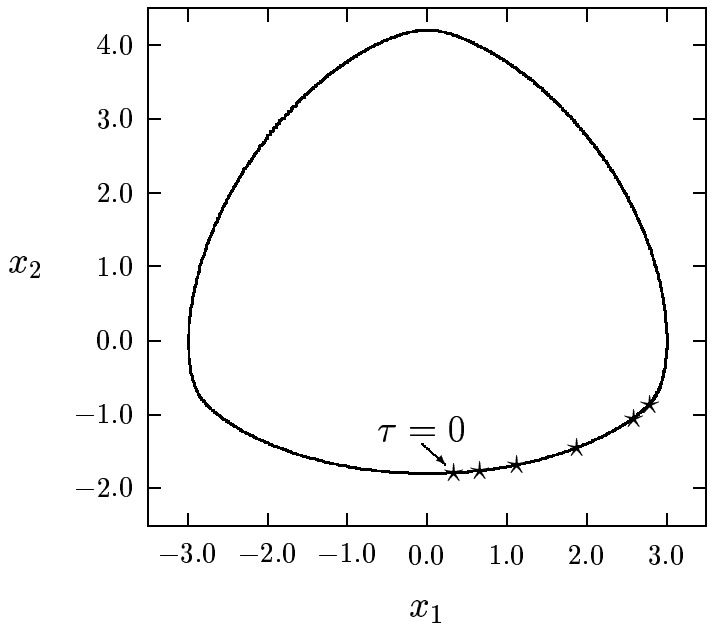


Figure 2: For Example 1 we plot the motion of the center of the spike on the boundary at different times as it tends to its steady-state limit. The initial point is labeled and the times corresponding to the other points (in counterclockwise order) are $\tau = 34.49$, $\tau = 58.71$, $\tau = 74.01$, $\tau = 76.98$ and $\tau = 77.50$.

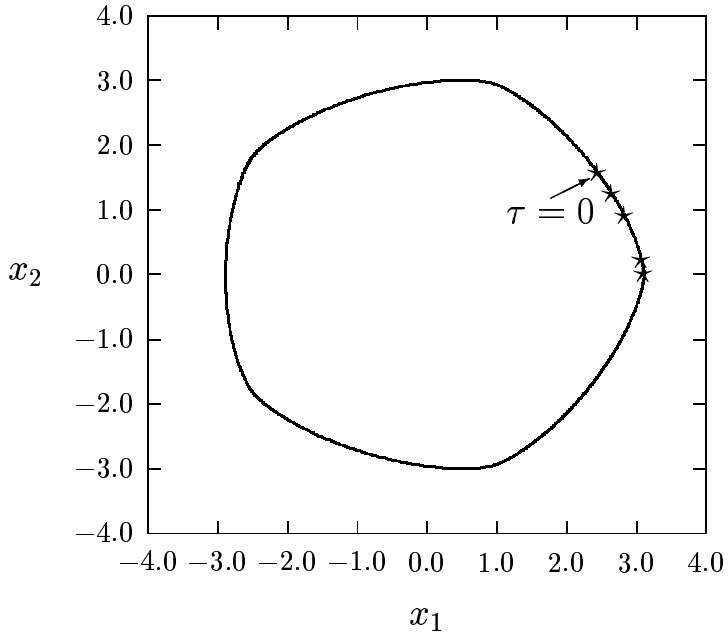


Figure 4: For Example 2 we plot the motion of the center of the spike on the boundary at different times as it tends to its steady-state limit. The initial point is labeled and the times corresponding to the other points (in clockwise order) are $\tau = 23.40$, $\tau = 31.41$, $\tau = 35.38$, and $\tau = 35.5$.

Hence there are five local maxima of the curvature. In Fig. 4 we plot the domain bounded by $\zeta(\theta)$ and show snapshots of the spike motion towards the nearby local maximum of the curvature at $\theta_0 = 0$. In Fig. 5 we plot the numerical solution to (2.24) with $\theta_0(0) = 0.6$. The apparent nonsmoothness of the graph of $\theta_0$ versus $\tau$ near the equilibrium point results from the fact that the linearization of (2.24) near $\theta_0 = 0$ has the form $\theta' \approx -c\theta$, where $c > 0$ is a large constant. A similar explanation hold for the apparent nonsmoothness in Fig. 3.

# 3 Spike Motion on the Boundary in Three Dimensions

We now derive an asymptotic differential equation for the motion of a spike confined to the boundary of a three-dimensional domain. The boundary of the domain is assumed to be sufficiently smooth so that the principal curvatures and their partial derivatives are continuous functions. In order to evaluate the Laplacian on the boundary we will use boundary layer coordinates. Lines of curvature form a local orthonormal basis for a coordinate system restricted to the boundary. We may then extend this system locally using the normal to the boundary as our third coordinate. The formulation of the Laplacian operator using these coordinates is not as simple as for the two-dimensional case. However, since the spike is localized on the boundary, we do not need an exact expression for the Laplacian in terms

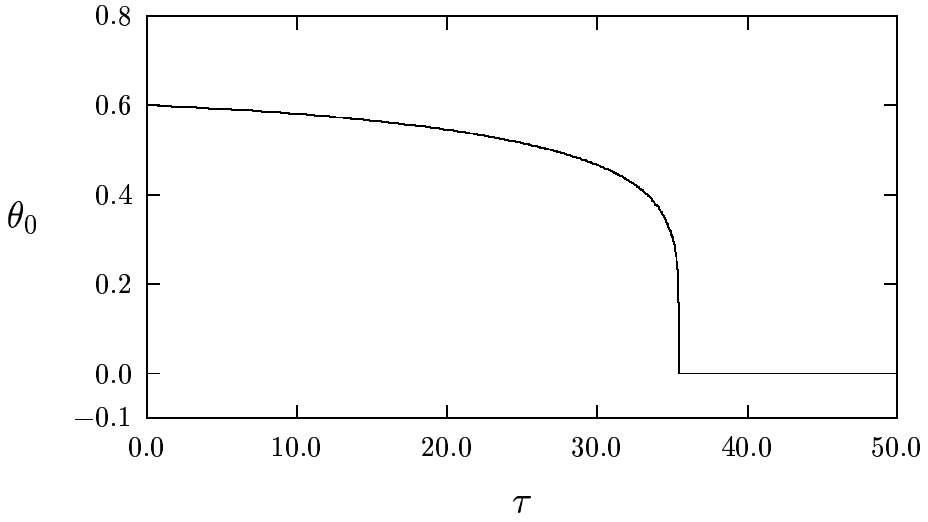


Figure 5: For Example 2 we plot the solution $\theta_0$ versus $\tau$ to (2.24) showing the behavior towards a local maximum of the curvature. The initial condition was $\theta_0(0) = 0.6$.

of these coordinates as only the first few terms in the local expansion will suffice for the analysis.

We introduce a boundary layer coordinate system $(s_1, s_2, \eta)$, where $\eta > 0$ is the distance from $\boldsymbol{x} \in D$ to $\partial D$ and where $s_1$ and $s_2$ correspond to coordinates through the two principal directions at the center of the spike. The boundary spike is assumed to be located at $s_1 = \xi_1(t)$ and $s_2 = \xi_2(t)$ with $\eta = 0$. Using Appendix A, we obtain that (1.3) transforms to

$$a_t = \epsilon^2 a_{\eta\eta} - \epsilon^2 \left( \frac{\kappa_1}{1-\eta\kappa_1} + \frac{\kappa_2}{1-\eta\kappa_2} \right) a_\eta + \frac{\epsilon^2}{(1-\eta\kappa_1)(1-\eta\kappa_2)} \partial_{s_1} \left( \frac{1-\eta\kappa_2}{1-\eta\kappa_1} a_{s_1} \right) + \frac{\epsilon^2}{(1-\eta\kappa_1)(1-\eta\kappa_2)} \partial_{s_2} \left( \frac{1-\eta\kappa_1}{1-\eta\kappa_2} a_{s_2} \right) - a + a^p/h^q \,, \tag{3.1a}$$

$$a_\eta = 0 \,, \qquad \text{on} \quad \eta = 0 \,. \tag{3.1b}$$

Here $\kappa_1 = \kappa_1(s_1, s_2)$ and $\kappa_2(s_1, s_2)$ are the two principal curvatures at each point on the boundary.

As in (2.2) we set $a = h^\gamma u$, where $u = u(\eta, s_1, s_2, t)$. Then, we introduce local coordinates $v$, $\hat{s}_1$, $\hat{s}_2$ and $\hat{\eta}$ by

$$\hat{s}_1 = \epsilon^{-1} \left[ s_1 - \xi_1(t) \right] \,, \qquad \hat{s}_2 = \epsilon^{-1} \left[ s_2 - \xi_2(t) \right] \,, \qquad \hat{\eta} = \epsilon^{-1} \eta \,,$$
$$v(\hat{\eta}, \hat{s}_1, \hat{s}_2, t) = u(\epsilon\hat{\eta}, \xi_1 + \epsilon\hat{s}_1, \xi_2 + \epsilon\hat{s}_2, t) \,. \tag{3.2}$$

The estimate (2.6) and the time scale (2.9) still apply in the three-dimensional case. Next,

we expand $v$ as in (2.7). The principal curvatures are also expanded in the Taylor series

$$\kappa_1(\xi_1+\epsilon\hat{s}_1,\xi_2+\epsilon\hat{s}_2)=\kappa_1+\epsilon\hat{s}_1\kappa_{11}+\epsilon\hat{s}_2\kappa_{12}+O(\epsilon^2)\,, \tag{3.3a}$$

$$\kappa_2(\xi_1+\epsilon\hat{s}_1,\xi_2+\epsilon\hat{s}_2)=\kappa_2+\epsilon\hat{s}_1\kappa_{21}+\epsilon\hat{s}_2\kappa_{22}+O(\epsilon^2)\,. \tag{3.3b}$$

Here on the right hand side of (3.3a) and (3.3b) we have defined $\kappa_1\equiv\kappa_1(\xi_1,\xi_2)$, $\kappa_2\equiv\kappa_2(\xi_1,\xi_2)$, and $\kappa_{ij}\equiv\partial_{s_j}\kappa_i(s_1,s_2)$ evaluated at $(s_1,s_2)=(\xi_1,\xi_2)$.

Substituting (2.6), (2.7), (2.9), (3.2) and (3.3) into (3.1), we obtain the following sequence of problems upon collecting powers of $\epsilon$:

$$v_{0\hat{\eta}\hat{\eta}}+v_{0\hat{s}_1\hat{s}_1}+v_{0\hat{s}_2\hat{s}_2}+Q(v_0)=0\,, \tag{3.4a}$$

$$\mathcal{L}v_1\equiv v_{1\hat{\eta}\hat{\eta}}+v_{1\hat{s}_1\hat{s}_1}+v_{1\hat{s}_2\hat{s}_2}+Q'(v_0)v_1=(\kappa_1+\kappa_2)v_{0\hat{\eta}}-2\hat{\eta}\kappa_1v_{0\hat{s}_1\hat{s}_1}-2\hat{\eta}\kappa_2v_{0\hat{s}_2\hat{s}_2}\,, \tag{3.4b}$$

$$\mathcal{L}v_2\equiv v_{2\hat{\eta}\hat{\eta}}+v_{2\hat{s}_1\hat{s}_1}+v_{2\hat{s}_2\hat{s}_2}+Q'(v_0)v_2=F_{ee}+F_{eo}+F_{oe}\,. \tag{3.4c}$$

The boundary conditions for (3.4) are

$$v_{0\hat{\eta}}=v_{1\hat{\eta}}=v_{2\hat{\eta}}=0\,,\qquad\text{on}\quad\hat{\eta}=0\,. \tag{3.4d}$$

In (2.10), $Q(v_0)$ is defined in (2.11). The terms $F_{ee}$, $F_{eo}$ and $F_{oe}$ in (3.4c) are defined by

$$\begin{aligned}F_{ee}=&-\frac{1}{2}Q''(v_0)v_1^2+(\kappa_1+\kappa_2)v_{1\hat{\eta}}+\hat{\eta}(\kappa_1^2+\kappa_2^2)v_{0\hat{\eta}}+\frac{\epsilon v_0\gamma\dot{h}}{h}\\&-2\hat{\eta}\kappa_1v_{1\hat{s}_1\hat{s}_1}-2\hat{\eta}\kappa_2v_{1\hat{s}_2\hat{s}_2}-3\kappa_1^2\hat{\eta}^2v_{0\hat{s}_1\hat{s}_1}-3\kappa_2^2\hat{\eta}^2v_{0\hat{s}_2\hat{s}_2}\,,\end{aligned} \tag{3.5a}$$

$$\begin{aligned}F_{eo}=&(\kappa_{12}+\kappa_{22})\hat{s}_2v_{0\hat{\eta}}-2\hat{\eta}\kappa_{12}\hat{s}_2v_{0\hat{s}_1\hat{s}_1}-2\hat{\eta}\kappa_{22}\hat{s}_2v_{0\hat{s}_2\hat{s}_2}\\&-\hat{\eta}(\kappa_{22}-\kappa_{12})v_{0\hat{s}_2}-\dot{\xi}_1v_{0\hat{s}_2}\,,\end{aligned} \tag{3.5b}$$

$$\begin{aligned}F_{oe}=&(\kappa_{21}+\kappa_{11})\hat{s}_1v_{0\hat{\eta}}-2\hat{\eta}\kappa_{11}\hat{s}_1v_{0\hat{s}_1\hat{s}_1}-2\hat{\eta}\kappa_{21}\hat{s}_1v_{0\hat{s}_2\hat{s}_2}\\&-\hat{\eta}(\kappa_{11}-\kappa_{21})v_{0\hat{s}_1}-\dot{\xi}_2v_{0\hat{s}_1}\,.\end{aligned} \tag{3.5c}$$

Here $\dot{\xi}_j\equiv d\xi_j/d\tau$ for $j=1,2$. The problems in (3.4) are to be solved in the half-space $\Omega$ defined by

$$\Omega=\{(\hat{\eta},\hat{s}_1,\hat{s}_2)\,|\,-\infty<\hat{s}_1<\infty\,,-\infty<\hat{s}_2<\infty\,,\hat{\eta}>0\}\,. \tag{3.6}$$

When $p$ is less than the critical Sobolev exponent $p_c=5$, there is a unique positive radially symmetric solution $u_c(\rho)$ to (3.5a) that satisfies (see [7])

$$u_c''+\frac{2}{\rho}u_c'+Q(u_c)=0\,,\qquad 0<\rho<\infty\,, \tag{3.7a}$$

$$u_c'(0)=0\,;\qquad u_c(\rho)\sim a_c\rho^{-1}e^{-\rho}\,,\qquad\text{as}\quad\rho\to\infty\,, \tag{3.7b}$$

for some $a_c>0$ where $\rho\equiv\left(\hat{\eta}^2+\hat{s}_1^2+\hat{s}_2^2\right)^{1/2}$. Therefore, our leading-order spike solution is given by

$$v_0(\hat{\eta},\hat{s}_1,\hat{s}_2)=u_c\left[(\hat{\eta}^2+\hat{s}_1^2+\hat{s}_2^2)^{1/2}\right]\,. \tag{3.8}$$

To obtain our solvability condition, we first define the inner product $(f,g)$ by $(f,g) \equiv \int_\Omega fg\, d\Omega$ where $\Omega$ is the half-space defined in (3.6). Then, we note that $\mathcal{L}v_{0\hat{s}_1} = 0$ and $\mathcal{L}v_{0\hat{s}_2} = 0$, where $\mathcal{L}$ is the operator defined in (3.4b), and that $v_{0\hat{s}_1}$ and $v_{0\hat{s}_2}$ satisfy the boundary condition in (3.4d). Therefore, the solvability condition is that the right hand sides of (3.4b) and (3.4c) must be orthogonal to both $v_{0\hat{s}_1}$ and $v_{0\hat{s}_2}$ with respect to this inner product.

In imposing the solvability condition on (3.4b), we note that the right hand side of (3.4b) is even in both $\hat{s}_1$ and $\hat{s}_2$, whereas $v_{0\hat{s}_1}$ is odd in $\hat{s}_1$ and even in $\hat{s}_2$, while $v_{0\hat{s}_2}$ is even in $\hat{s}_1$ and odd in $\hat{s}_2$. Hence, the solvability condition for (3.4b) is automatically satisfied. Then, from (3.4b) together with (3.4d) we can calculate a function $v_1$, which is even in both $\hat{s}_1$ and $\hat{s}_2$. Next, the solvability condition for (3.4c) yields the two equations

$$(F_{ee}, v_{0\hat{s}_1}) + (F_{eo}, v_{0\hat{s}_1}) + (F_{oe}, v_{0\hat{s}_1}) = 0\,, \qquad (F_{ee}, v_{0\hat{s}_2}) + (F_{eo}, v_{0\hat{s}_2}) + (F_{oe}, v_{0\hat{s}_2}) = 0\,. \tag{3.9}$$

The significance of the decomposition in (3.4c) is that $F_{ee}$ is even in both $\hat{s}_1$ and $\hat{s}_2$, $F_{eo}$ is even in $\hat{s}_1$ and odd in $\hat{s}_2$, and $F_{oe}$ is odd in $\hat{s}_1$ and even in $\hat{s}_2$. Therefore, the inner products involving $F_{ee}$ vanish, and also $(F_{eo}, v_{0\hat{s}_1}) = (F_{oe}, v_{0\hat{s}_2}) = 0$. Using these results, and substituting (3.5b) and (3.5c) into (3.9) we obtain

$$\begin{aligned}\dot{\xi}_1 \left(v_{0\hat{s}_1}, v_{0\hat{s}_1}\right) &= (\kappa_{21}+\kappa_{11}) \left(\hat{s}_1 v_{0\hat{\eta}}, v_{0\hat{s}_1}\right) - 2\kappa_{11} \left(\hat{\eta}\hat{s}_1 v_{0\hat{s}_1\hat{s}_1}, v_{0\hat{s}_1}\right) \\ &\quad - 2\kappa_{21} \left(\hat{\eta}\hat{s}_1 v_{0\hat{s}_2\hat{s}_2}, v_{0\hat{s}_1}\right) - (\kappa_{11}-\kappa_{21}) \left(\hat{\eta} v_{0\hat{s}_1}, v_{0\hat{s}_1}\right)\,, \qquad (3.10a)\\ \dot{\xi}_2 \left(v_{0\hat{s}_2}, v_{0\hat{s}_2}\right) &= (\kappa_{12}+\kappa_{22}) \left(\hat{s}_2 v_{0\hat{\eta}}, v_{0\hat{s}_2}\right) - 2\kappa_{12} \left(\hat{\eta}\hat{s}_2 v_{0\hat{s}_1\hat{s}_1}, v_{0\hat{s}_2}\right) \\ &\quad - 2\kappa_{22} \left(\hat{\eta}\hat{s}_2 v_{0\hat{s}_2\hat{s}_2}, v_{0\hat{s}_2}\right) - (\kappa_{22}-\kappa_{12}) \left(\hat{\eta} v_{0\hat{s}_2}, v_{0\hat{s}_2}\right)\,. \qquad (3.10b)\end{aligned}$$

We now evaluate the inner products in (3.10). We first integrate by parts to get

$$2\left(\hat{\eta}\hat{s}_j v_{0\hat{s}_j\hat{s}_j}, v_{0\hat{s}_j}\right) = -\left(\hat{\eta}, [v_{0\hat{s}_j}]^2\right)\,, \qquad j=1,2\,. \tag{3.11a}$$

Next, we use spherical coordinates to obtain

$$\left(\hat{\eta} v_{0\hat{s}_j}, v_{0\hat{s}_j}\right) = \frac{\pi}{4}\int_0^\infty \rho^3 \left[u_c'(\rho)\right]^2 d\rho\,, \qquad j=1,2\,, \tag{3.11b}$$

$$\left(v_{0\hat{s}_j}, v_{0\hat{s}_j}\right) = \frac{2\pi}{3}\int_0^\infty \rho^2 \left[u_c'(\rho)\right]^2 d\rho\,, \qquad j=1,2\,, \tag{3.11c}$$

$$\left(\hat{s}_j v_{0\hat{\eta}}, v_{0\hat{s}_j}\right) = \frac{\pi}{4}\int_0^\infty \rho^3 \left[u_c'(\rho)\right]^2 d\rho\,, \qquad j=1,2\,, \tag{3.11d}$$

$$(\hat{\eta}\hat{s}_2 v_{0\hat{s}_1\hat{s}_1}, v_{0\hat{s}_2}) = (\hat{\eta}\hat{s}_1 v_{0\hat{s}_2\hat{s}_2}, v_{0\hat{s}_1}) = \frac{\pi}{8}\int_0^\infty \rho^3 \left[u_c'(\rho)\right]^2 d\rho\,. \tag{3.11e}$$

Then, substituting (3.11) into (3.10) we obtain,

$$\dot{\xi}_1 = \frac{3b}{8}(\kappa_{21}+\kappa_{11})\,, \qquad \dot{\xi}_2 = \frac{3b}{8}(\kappa_{22}+\kappa_{12})\,, \tag{3.12a}$$

where $b > 0$ is defined by

$$b = \frac{\int_0^\infty \rho^3 \left[u_c'(\rho)\right]^2 \, d\rho}{\int_0^\infty \rho^2 \left[u_c'(\rho)\right]^2 \, d\rho} \,. \tag{3.12b}$$

Finally, upon introducing the mean curvature $H(\xi_1, \xi_2)$ defined by $H = (\kappa_1 + \kappa_2)/2$, we obtain the main result.

**Proposition 3.1**: *For $\epsilon \to 0$, the motion of a spike confined to the smooth boundary of a three-dimensional domain is described by*

$$a \sim h^\gamma u_c \left( \epsilon^{-1} \left[ (s_1 - \xi_1(t))^2 + (s_2 - \xi_2(t))^2 + \eta^2 \right]^{1/2} \right) + O(\epsilon) \,, \tag{3.13a}$$

$$\boldsymbol{\xi}'(t) \sim \frac{3}{4} b \epsilon^3 \boldsymbol{\nabla} H(\boldsymbol{\xi}) \,. \tag{3.13b}$$

*Here $\boldsymbol{\xi} = (\xi_1, \xi_2)$, $\gamma = q/(p-1)$, $b > 0$ is defined in (3.12b), $u_c(\rho)$ is the positive solution to (3.7), and $H$ is the mean curvature of $\partial D$, with $H > 0$ for a sphere.* Notice that the stable equilibrium points of (3.13b) are at local maxima of the mean curvature.

Using the boundary value problem solver COLSYS [2] we can solve (3.7) numerically to determine the constant $b$ in (3.13b). In particular, when $p = 2$ we compute that

$$\int_0^\infty \rho^3 \left[u_c'(\rho)\right]^2 \, d\rho = 17.36 \,, \qquad \int_0^\infty \rho^2 \left[u_c'(\rho)\right]^2 \, d\rho = 10.42 \,. \tag{3.14}$$

Hence, when $p = 2$, we get $b = 1.67$.

# 4 Qualitative Properties of the Associated Eigenvalue Problem

In this section we qualitatively explain why the nonlocal term in (1.3) is essential for ensuring the existence of slow boundary spike motion.

We first consider the *local* problem corresponding to (1.3) in which we delete (1.3b) and fix $h > 0$. Let us suppose for the moment that the boundary is flat and is given by the coordinate line $x_N = 0$. Hence we take $D = \{\mathbf{x} = (x_1, \ldots, x_N) \,|\, x_N \geq 0\}$. Setting $a = h^{q/(p-1)} u$, we then get

$$u_t = \epsilon^2 \triangle u - u + u^p \,, \qquad x_N \geq 0 \,; \qquad \partial_{x_N} u = 0 \,, \qquad \text{on} \quad x_N = 0 \,. \tag{4.1}$$

Let $u = u_c\left(\epsilon^{-1}|\mathbf{x}|\right)$, where $u_c$ is the canonical spike solution defined in (2.13) and (3.7) for $N = 2$ and $N = 3$, respectively. We linearize (4.1) around $u_c$ by writing $u = u_c\left(\epsilon^{-1}|\mathbf{x}|\right) + \psi\left(\epsilon^{-1}|\mathbf{x}|\right) e^{\mu t}$. This leads to the local eigenvalue problem for $\psi(\mathbf{y})$ and $\mu$ on a flat boundary

$$\triangle' \psi + \left(-1 + p u_c^{p-1}\right) \psi = \mu \psi \,, \qquad y_N \geq 0 \,, \tag{4.2a}$$

$$\partial_{y_N} \psi = 0 \,, \qquad \text{on} \quad y_N = 0 \,. \tag{4.2b}$$

Here $\mathbf{y} = \epsilon^{-1}\mathbf{x}$, $u_c = u_c(|\mathbf{y}|)$ and $\triangle'$ denotes the Laplacian in the $\mathbf{y}$ variable. The eigenvalues $\mu_j$ of (4.2) satisfy

$$\mu_1 > 0\,,\ \mu_2 = \ldots = \mu_N = 0\,,\ \mu_{N+1} < 0\,. \tag{4.3}$$

The positivity of $\mu_1$ was shown in [13] and [19]. The eigenfunctions $\psi_1$ and $\psi_{N+1}$ are radially symmetric (i. e. $\psi_1 = \psi_1(|\mathbf{y}|)$). A numerical procedure to calculate $\mu_1$ was given in [19] and the results are shown in Table 1. The translation eigenfunctions corresponding to the zero eigenvalues are given by $\psi_j = \partial_{y_{j-1}} u_c(|\mathbf{y}|)$ for $j = 2, \ldots, N$.

| $p$ | $\mu_1(N=2)$ | $\mu_1(N=3)$ |
|---|---|---|
| 2 | 1.65 | 2.36 |
| 3 | 5.41 | 15.29 |
| 4 | 13.23 | 144.18 |

Table 1: Numerical results for the principal eigenvalue $\mu_1$ of the local problem on a flat boundary (4.2).

The *local* eigenvalue problem on a *curved* boundary has the form

$$\mathcal{A}_\epsilon \psi^\epsilon + \left(-1 + p u_c^{p-1}\right)\psi^\epsilon = \mu^\epsilon \psi^\epsilon\,, \qquad \hat{\eta} \geq 0\,, \tag{4.4a}$$

$$\partial_{\hat{\eta}} \psi^\epsilon = 0\,, \qquad \text{on} \quad \hat{\eta} = 0\,. \tag{4.4b}$$

Here $\mathcal{A}_\epsilon$ is the operator that results from converting the Laplacian into local boundary coordinates as explained in §2 and §3. Clearly, $\mathcal{A}_\epsilon \to \triangle'$ as $\epsilon \to 0$. Hence, we would expect that the eigenvalues of (4.2) and (4.4) are close as $\epsilon \to 0$. In fact, it was proved in [21] that, for $\epsilon \ll 1$, the eigenvalues $\mu_j^\epsilon$ of (4.4) satisfy

$$\mu_j^\epsilon = \mu_j + o(1)\,, \qquad j = 1, \ldots, N+1, \ldots\,. \tag{4.5}$$

Hence, $\mu_1^\epsilon > 0$ for $\epsilon$ sufficiently small. This shows that a boundary spike solution for the local problem corresponding to (1.3) will not drift slowly along the boundary of the domain. The eigenvalues $\mu_2^\epsilon, \ldots, \mu_N^\epsilon$ corresponding to the near translation modes were calculated for $\epsilon \ll 1$ in [21].

Next, we linearize the *nonlocal problem* (1.3) around a spike solution centered on a flat boundary. In place of (4.2), we obtain the nonlocal eigenvalue problem for $\lambda$ and $\phi$ given by

$$\triangle'\phi + \left(-1 + p u_c^{p-1}\right)\phi + I(\phi) = \lambda\phi\,, \qquad y_N \geq 0\,, \tag{4.6a}$$

$$\partial_{y_N}\phi = 0\,, \qquad \text{on} \quad y_N = 0\,, \tag{4.6b}$$

where $I(\phi)$ is defined by

$$I(\phi) \equiv -\frac{2mqu_c^p}{\Omega_N \beta(s+1)} \int_D u_c^{m-1}\phi\, d\mathbf{y}\,, \qquad \beta \equiv \int_0^\infty [u_c(\rho)]^m\, \rho^{N-1}\, d\rho\,. \tag{4.6c}$$

Here $D$ is the half-space $y_N \geq 0$, $\Omega_N$ is the surface area of the unit $N$-dimensional sphere, and $u_c = u_c(|\mathbf{y}|)$.

As is similar to (4.5), the eigenvalues of the nonlocal problem defined on a curved boundary should be asymptotically close to within $o(1)$ terms to the eigenvalues of (4.6). Hence, to ensure the existence of slow boundary spike motion for (1.3) we need only show that all of the eigenvalues of (4.6) satisfy $\mathrm{Re}(\lambda) \leq 0$.

In [10] a homotopy method was used to compute eigenvalues of (4.6) corresponding to radially symmetric eigenfunctions. In this procedure we replaced $I(\phi)$ in (4.6a) with $\delta I(\phi)$ where $\delta$, satisfying $0 \leq \delta \leq 1$, is a continuation parameter. We then calculated the branches of eigenvalues of (4.6) as a function of $\delta$ that emanate from the eigenvalues $\mu_1$ and $\mu_{N+1}$ of the local problem when $\delta = 0$. The results of these computations for the parameter set $p = 2$, $q = 1$, $m = 2$ and $s = 0$ are shown in Fig. 8, Fig. 9 and Table 2 of [10]. These computations showed that the nonlocal term has pushed these eigenvalues into the left half-plane when $\delta = 1$. Similar conclusions were found with other parameter sets. Hence, the unstable eigenvalue $\mu_1$ associated with the local problem (4.2) has been eliminated by the presence of the nonlocal term $I(\phi)$. A rigorous result proving this assertion for a wide range of parameter values $p$ and $r$ is given in [20].

Finally, we note that the problem (4.6) preserves the translation eigenvalues associated with the local problem (4.2), since by symmetry the nonlocal term $I(\phi)$ satisfies $I\left(\partial_{y_{j-1}} u_c\right) = 0$ for $j = 2, \ldots, N$. As is similar to (4.5), these translation eigenvalues are perturbed by $o(1)$ as $\epsilon \to 0$ when the nonlocal eigenvalue problem is defined on a curved boundary. The resulting small eigenvalues are responsible for the slow boundary spike motion derived in §2 and §3.

# 5 A Spike on a Flat Boundary in Two Dimensions

In §2 we showed that the motion of a spike centered on the boundary of a two-dimensional domain is in the direction of increasing curvature. This leads us to the problem of determining the motion of a spike when the curvature is constant. In particular, we will analyze the motion of a spike on a flat boundary where the curvature vanishes. Our analysis below shows that this motion is metastable. To obtain this result, in §5.1 we show that the principal eigenvalue associated with the linearization of a spike solution centered on a flat boundary is exponentially small. This establishes the metastability. Then, in §5.2 we derive an asymptotic differential equation for the metastable spike motion on the flat boundary by imposing a limiting solvability condition on the solution to the linearized problem. This condition ensures that this linearized solution is orthogonal to the eigenfunction associated with the exponentially small eigenvalue.

For the analysis we let $\mathbf{x} = (x, y)$ and we suppose that the spike is located on the straight-line boundary segment joining the points $(x_L, 0)$ and $(x_R, 0)$ as shown in Fig. 6. The flat portion of $\partial D$ is taken to be the straight-line segment between $(x_L, 0)$ and $(x_R, 0)$. The spike is centered at $\mathbf{x}_0 = (\xi, 0)$ where $x_L < \xi < x_R$. We decompose $\partial D$ as $\partial D = \partial D_c \cup \partial D_s$ where

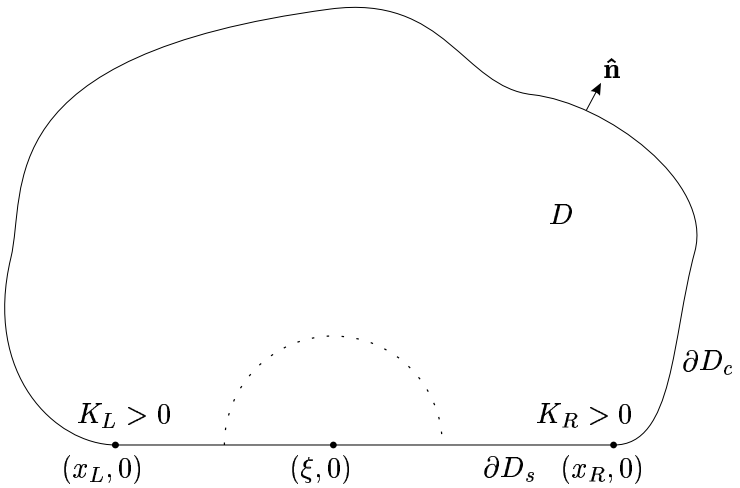


Figure 6: Plot of a two-dimensional domain $D$ with a flat boundary segment. The spike is centered at $x = \xi$ on the flat segment. The dotted line indicates an approximate equipotential for $u$.

$\partial D_s$ refers to the straight-line segment of the boundary and $\partial D_c$ denotes the remaining curved part of $\partial D$. The distance between the spike and $\partial D_c$ is assumed to be a minimum at either of the two corners $(x_L, 0)$ or $(x_R, 0)$.

The local behavior of the boundary near the corner points is critical to our analysis. Near the corner points, $\partial D_c$ is assumed to have the local behavior

$$\text{near } (x_L,0)\,; \quad y = \psi_L(x), \qquad \psi_L'(x) \sim -K_L(x_L - x)^{\alpha_L}\,, \quad \text{as } x \to x_L^-, \tag{5.1a}$$

$$\text{near } (x_R,0)\,; \quad y = \psi_R(x), \qquad \psi_R'(x) \sim K_R(x - x_R)^{\alpha_R}\,, \quad \text{as } x \to x_R^+, \tag{5.1b}$$

where $\alpha_L > 0$ and $\alpha_R > 0$. When $\alpha_L = \alpha_R = 1$, $K_L$ and $K_R$ are proportional to the curvature of $\partial D_c$ at the left and right corners, respectively.

The spike solution to (1.3) is given asymptotically by

$$a(\mathbf{x}, t) \sim a_e \equiv h_e^{q/(p-1)} u_c\left(\epsilon^{-1}|\mathbf{x} - \mathbf{x}_0(t)|\right)\,, \tag{5.2a}$$

$$h \sim h_e \equiv \left(\frac{\pi}{\mu|D|}\int_0^\infty [u_c(\rho)]^m\,\rho\,d\rho\right)^{\frac{p-1}{(s+1)(p-1)-qm}}\,, \tag{5.2b}$$

where $\mathbf{x}_0(t) = (\xi(t), 0)$ is to be determined. Here $u_c(\rho)$ is the radially symmetric solution defined in (2.13), and $|D|$ denotes the area of $D$.

We first linearize (1.3) around $a_e$ by writing $a = a_e + v$, where $v \ll a_e$. We get that $v$ satisfies,

$$\mathcal{L}_\epsilon v \equiv \epsilon^2\Delta v + (-1 + p u_c^{p-1})v - \frac{mq\epsilon^{-2}u_c^p}{\pi\beta(s+1)}\int_D u_c^{m-1} v\,d\mathbf{x} = v_t + \partial_t a_e\,, \quad \text{in} \quad D\,, \tag{5.3a}$$

$$\partial_n v = -\partial_n a_e \quad \text{on} \quad \partial D\,. \tag{5.3b}$$

Here $\beta$ is defined by

$$\beta = \int_0^\infty [u_c(\rho)]^m\,\rho\,d\rho\,. \tag{5.4}$$

Now we let $v = e^{\lambda t}\phi$ to get the eigenvalue problem,

$$\mathcal{L}_\epsilon \phi = \lambda \phi\,, \quad \text{in} \quad D\,; \qquad \partial_n \phi = 0 \quad \text{on} \quad \partial D\,. \tag{5.5}$$

### 5.1 The Translation Eigenvalue

Suppose for the moment that $D$ is the half-space $y \geq 0$ so that $\partial D_s$ is the entire $x$-axis. Then, the function $\tilde{\phi} \equiv \partial_x u_c$ satisfies $\mathcal{L}_\epsilon \tilde{\phi} = 0$ and the normal derivative boundary condition $\partial_n \tilde{\phi} = 0$. Hence, for this case, $\tilde{\phi}$ is an eigenfunction of $\mathcal{L}$ with a zero eigenvalue. This corresponds to translation invariance in the $x$ direction. For our geometry, $\tilde{\phi}$ is localized near $(\xi, 0)$ on the flat segment $\partial D_s$ and $\tilde{\phi}$ decays exponentially away from this point. The interaction of the exponentially small far-field behavior of $\tilde{\phi}$ with the corner regions, where $\partial D_s$ and $\partial D_c$ meet, perturbs the zero eigenvalue by exponentially small terms. This shift in the zero eigenvalue is calculated below. The nonlocal term in the operator $\mathcal{L}_\epsilon$ is asymptotically negligible in the calculation of this shift. However, as shown in §4, the nonlocal term is essential for ensuring that the translation eigenvalue is the principal eigenvalue of the linearization.

Now we calculate $\lambda_1$ and $\phi_1$. Since $\tilde{\phi}$ fails to satisfy the boundary condition on $\partial D_c$, the principal eigenfunction $\phi_1$ has the form

$$\phi_1 \sim C_1 \left(\partial_x u_c + \phi_L\right)\,. \tag{5.6}$$

Here $C_1$ is a normalization constant and $\phi_L$ is a boundary layer correction term localized near $\partial D_c$. Let $\eta < 0$ be the distance between $\boldsymbol{x} \in D$ and $\partial D$ and let $\hat{\eta} = \epsilon^{-1}\eta$ be the localized coordinate. Then, from (5.5), we get that $\phi_L$ satisfies

$$\phi_{L\hat{\eta}\hat{\eta}} - \phi_L = 0, \qquad \hat{\eta} < 0\,, \tag{5.7a}$$

$$\partial_{\hat{\eta}} \phi_L = -\epsilon \partial_{\hat{\eta}} [\partial_x u_c]|_{\hat{\eta}=0}\,, \quad \text{on} \quad \hat{\eta} = 0\,; \qquad \phi_L \to 0\,, \quad \text{as} \quad \hat{\eta} \to -\infty\,. \tag{5.7b}$$

The solution to (5.7) is

$$\phi_L = -\epsilon \left(\partial_{\hat{\eta}} [\partial_x u_c]|_{\hat{\eta}=0}\right) e^{\eta/\epsilon}\,. \tag{5.8}$$

Since $u_c$ is localized near $x = \xi \in \partial D_s$, we can calculate $\phi_1$ and $\phi_L$ on $\partial D_c$ by using the far-field behavior of $u_c$ given in (2.13b). In this way, we get an estimate for $\phi_1$ on $\partial D_c$ from (5.6) and (5.8)

$$\phi_1 \sim -C_1 a_c \epsilon^{-1/2} r^{-3/2} (x - \xi) e^{-r/\epsilon} \left(1 + \hat{\mathbf{r}} \cdot \hat{\mathbf{n}}\right)\,, \quad \text{on} \quad \partial D_c\,. \tag{5.9}$$

Here $a_c$ is defined in (2.13b), $r = |\boldsymbol{x} - \mathbf{x}_0|$, $\mathbf{r} = (\boldsymbol{x} - \mathbf{x}_0)/r$, and $\mathbf{n}$ is the unit outward normal to $\partial D_c$.

Applying Green's identity to $\phi_1$ and $\partial_x u_c$, and using the facts that $\partial_n \phi_1 = 0$ on $\partial D$ and $\partial_n [\partial_x u_c] = 0$ on $\partial D_s$, we obtain

$$\lambda_1 \left(\partial_x u_c, \phi_1\right) = -\epsilon^2 \int_{\partial D_c} \phi_1 \partial_n [\partial_x u_c]\, dS + \left(\mathcal{L}_\epsilon^* [\partial_x u_c], \phi_1\right)\,. \tag{5.10}$$

Here $(f,g) \equiv \int_D fg\, d\mathbf{x}$ and $\mathcal{L}_\epsilon^*$ is the adjoint operator defined by

$$\mathcal{L}_\epsilon^* \phi \equiv \epsilon^2 \Delta \phi - \phi + u_c^{p-1}\phi - \frac{mq\epsilon^{-2}u_c^{m-1}}{\beta\pi(s+1)} \int_D u_c^p \phi \, d\mathbf{x} \,. \tag{5.11}$$

We now estimate each term in (5.10). Using polar coordinates, we calculate

$$(\phi_1, \partial_x u_c) \sim \frac{\pi C_1 \gamma}{2} \,, \qquad \text{where} \quad \gamma \equiv \int_0^\infty \rho \left[ u_c'(\rho) \right]^2 d\rho \,. \tag{5.12}$$

Next, we use (5.9) and the far-field form of $u_c$ in (2.13b) to get

$$\phi_1 \partial_n \left[ \partial_x u_c \right] \sim -\frac{C_1 a_c^2 \epsilon^{-2}}{r} \left( \frac{x-\xi}{r} \right)^2 e^{-2r/\epsilon} \hat{\mathbf{r}} \cdot \hat{\mathbf{n}} \left( 1 + \hat{\mathbf{r}} \cdot \hat{\mathbf{n}} \right) \,, \qquad \text{on} \quad \partial D_c \,. \tag{5.13}$$

Substituting (5.13) into the boundary integral in (5.10), we observe that the dominant contribution to this integral arises from the corner regions of $\partial D_c$, where $r$ is the smallest. Near the corner regions we use the local behavior (5.1) to calculate

$$\hat{\mathbf{r}} \cdot \hat{\mathbf{n}} \sim \begin{cases} K_L (x_L - x)^{\alpha_L} \,, & \text{as} \quad x \to x_L^- \\ K_R (x - x_R)^{\alpha_R} \,, & \text{as} \quad x \to x_R^+ \,. \end{cases} \tag{5.14}$$

Substituting (5.13) and (5.14) into the boundary integral in (5.10), and using Laplace's method, we get

$$\begin{aligned} B \equiv -\epsilon^2 \int_{\partial D_c} \phi_1 \partial_n [\partial_x u_c] \, dS \sim C_1 a_c^2 \int_{-\infty}^{x_L} \frac{K_L (x_L - x)^{\alpha_L}}{\xi - x_L} \, e^{-2(\xi - x)/\epsilon} \, dx \,, \\ + C_1 a_c^2 \int_{x_R}^{\infty} \frac{K_R (x - x_R)^{\alpha_R}}{x_R - \xi} \, e^{-2(x-\xi)/\epsilon} \, dx \,. \end{aligned} \tag{5.15}$$

The integrals in (5.15) are evaluated explicitly by using

$$\int_0^\infty z^\alpha e^{-2z/\epsilon} \, dz = \left( \frac{\epsilon}{2} \right)^{\alpha+1} \Gamma(\alpha+1) \,, \tag{5.16}$$

where $\Gamma(z)$ is the Gamma function. In this way, (5.15) becomes

$$\begin{aligned} B \sim C_1 a_c^2 \left\{ \frac{K_R}{x_R - \xi} \left( \frac{\epsilon}{2} \right)^{\alpha_R + 1} \Gamma(\alpha_R + 1) \, e^{-2(x_R - \xi)/\epsilon} \right. \\ \left. + \frac{K_L}{\xi - x_L} \left( \frac{\epsilon}{2} \right)^{\alpha_L + 1} \Gamma(\alpha_L + 1) \, e^{-2(\xi - x_L)/\epsilon} \right\} \,. \end{aligned} \tag{5.17}$$

Finally, in Appendix B we give asymptotic estimates to show that $(\mathcal{L}_\epsilon^* [\partial_x u_c] \,, \phi_1) = o(B)$, as $\epsilon \to 0$. Hence, we can neglect the last term on the right side of (5.10). Substituting (5.12) and (5.17) into (5.10), we get the following key asymptotic formula for the principal eigenvalue of (5.5):

**Proposition 5.1 (Eigenvalue)**: *Assume that the distance between $\xi$ and $\partial D_c$ is a minimum at either of the two corners $(x_L, 0)$ or $(x_R, 0)$. Then, for $\epsilon \to 0$, the principal eigenvalue $\lambda_1$ of (5.5) has the asymptotic estimate*

$$\begin{aligned} \lambda_1 \sim \frac{2a_c^2}{\pi\gamma} \left\{ \frac{K_R}{x_R - \xi} \left( \frac{\epsilon}{2} \right)^{\alpha_R + 1} \Gamma(\alpha_R + 1) \, e^{-2(x_R - \xi)/\epsilon} \right. \\ \left. + \frac{K_L}{\xi - x_L} \left( \frac{\epsilon}{2} \right)^{\alpha_L + 1} \Gamma(\alpha_L + 1) \, e^{-2(\xi - x_L)/\epsilon} \right\} \,. \end{aligned} \tag{5.18}$$

*Here $a_c$ is given in (2.13b), $\gamma$ is defined in (5.12), and $K_L$, $K_R$, $\alpha_L$ and $\alpha_R$ are defined in (5.1) in terms of the local behavior of $\partial D_c$ near the corners.*

## 5.2 The Slow Spike Motion

We now derive a differential equation for $\xi(t)$ for the time-dependent problem. We assume that the spike is initially on $\partial D_s$. Then, since the spike motion is metastable we have $v_t \ll \partial_t a_e$ in (5.3a). Multiplying (5.3a) by $\phi_1$, and using $\partial_n \phi_1 = 0$ on $\partial D$, we obtain upon integration by parts that

$$(\mathcal{L}_\epsilon v, \phi_1) \sim \epsilon^2 \int_{\partial D} \phi_1 \partial_n v \, dS + (\mathcal{L}_\epsilon^* \phi_1, v) \ . \tag{5.19}$$

From (5.3) we have $\mathcal{L}_\epsilon v \sim \partial_t a_e$ in $D$, and $\partial_n v = -\partial_n a_e$ on $\partial D$, where $\partial_n a_e = 0$ on $\partial D_s$. Thus, (5.19) reduces to

$$(\partial_t u_c, \phi_1) \sim -\epsilon^2 \int_{\partial D_c} \phi_1 \partial_n u_c \, dS + h_e^{-q/(p-1)} \, (\mathcal{L}_\epsilon^* \phi_1, v) \ . \tag{5.20}$$

Similar estimates to those given in Appendix B, which we omit, shows that the last term on the right-hand side of (5.20) is negligible as compared to the boundary integral term. Hence,

$$(\partial_t u_c, \phi_1) \sim -\epsilon^2 \int_{\partial D_c} \phi_1 \partial_n u_c \, dS \, , \tag{5.21}$$

where $u_c = u_c \left[ \epsilon^{-1} |\boldsymbol{x} - \mathbf{x}_0| \right]$ and $\mathbf{x}_0(t) = (\xi(t), 0)$.

The remaining part of the analysis is very similar to the derivation of the eigenvalue estimate for $\lambda_1$, and hence we omit many of the details. For $\epsilon \ll 1$, we calculate using (5.6) that

$$(\partial_t u_c, \phi_1) \sim -\frac{\pi C_1 \xi' \gamma}{2} \, , \tag{5.22}$$

where $\gamma$ was defined in (5.12). Next, using the far-field behavior of $u_c$ given in (2.13b), the estimate for $\phi_1$ on $\partial D_c$ given in (5.9), and Laplace's method, the boundary integral in (5.21) can be evaluated asymptotically as in (5.13)–(5.17). The following main result is obtained from this calculation:

**Proposition 5.2 (Spike Motion)**: *Assume that the distance between $\xi$ and $\partial D_c$ is a minimum at either of the two corners $(x_L, 0)$ or $(x_R, 0)$. Then, for $\epsilon \to 0$, the $x$-coordinate of the center of the spike along the flat segment $\partial D_s$, denoted by $\xi(t)$, satisfies the asymptotic differential equation,*

$$\xi'(t) \sim \frac{2\epsilon a_c^2}{\pi \gamma} \left\{ \frac{K_R}{x_R - \xi} \left( \frac{\epsilon}{2} \right)^{\alpha_R + 1} \Gamma(\alpha_R + 1) \, e^{-2(x_R - \xi)/\epsilon} \right.$$
$$\left. - \frac{K_L}{\xi - x_L} \left( \frac{\epsilon}{2} \right)^{\alpha_L + 1} \Gamma(\alpha_L + 1) \, e^{-2(\xi - x_L)/\epsilon} \right\} . \tag{5.23}$$

*Here $a_c$ is given in (2.13b), $\gamma$ is defined in (5.12), and $K_L$, $K_R$, $\alpha_L$ and $\alpha_R$ are defined in (5.1) in terms of the local behavior of $\partial D_c$ near the corners.*

A similar differential equation for the motion of a straight-line interface in a constant width neck region of a dumbell-shaped domain has been derived in [12] for the Allen-Cahn equation. Using the boundary value problem solver COLSYS [2] we can solve (2.13) numerically to determine the constants $a_c$ and $\gamma$ in (5.18) and (5.23). In this way, when $p = 2$ we compute that $a_c = 10.80$ and $\gamma = 2.47$.

The result (5.23) shows that the motion of the spike along the straight-line boundary segment between $(x_L, 0)$ and $(x_R, 0)$ is determined by the shape of the boundary at $(x_L, 0)$ and $(x_R, 0)$ and by the distance between the spike and the corner regions. The spike will move according to (5.23) until a stable steady state is reached or until the spike touches $(x_L, 0)$ or $(x_R, 0)$. Once the spike reaches the curved part of the boundary $\partial D_c$, it will subsequently evolve according to (2.19b).

From (5.23), the steady-state spike-layer location $\xi_e$ on $\partial D_s$ satisfies

$$\frac{\xi_e - x_L}{x_R - \xi_e} e^{4\xi_e/\epsilon} = \frac{K_L \Gamma(\alpha_L + 1)}{K_R \Gamma(\alpha_R + 1)} \left(\frac{\epsilon}{2}\right)^{\alpha_L - \alpha_R} e^{2(x_R + x_L)/\epsilon} . \tag{5.24}$$

Since the left hand side of (5.24) increases from 0 to $\infty$ as $\xi_e$ ranges from $x_L$ to $x_R$, a unique steady-state solution to (5.24) exists on $x_L < \xi < x_R$ whenever $K_L$ and $K_R$ have the same sign. This solution is stable when $K_L < 0$ and $K_R < 0$, and is unstable when $K_L > 0$ and $K_R > 0$. In particular, this implies that if $D$ is convex near $(x_L, 0)$ and $(x_R, 0)$, then there is no stable equilibrium spike location on $\partial D_s$. A simple calculation using (5.24) shows that the equilibrium spike-layer location $\xi_e$, when it exists, has the expansion

$$\xi_e \sim \frac{x_L + x_R}{2} + \frac{\epsilon}{4} \log \left[ \frac{K_L \Gamma(\alpha_L + 1)}{K_R \Gamma(\alpha_R + 1)} \left(\frac{\epsilon}{2}\right)^{\alpha_L - \alpha_R} \right] + \cdots . \tag{5.25}$$

Thus, the equilibrium location, $\xi_e$ is located at an $O(\epsilon)$ distance from the midpoint of the straight-line boundary segment.

The following dynamical behavior can be deduced from (5.23) and (5.25) when the initial condition is $\xi(0) = \xi_0$. When $K_L > 0$ and $K_R > 0$, $\xi(t)$ will move monotonically towards $x_L$ if $\xi_0 < \xi_e$, or monotonically towards $x_R$ if $\xi_0 > \xi_e$ (see Fig. 7). When $K_L < 0$ and $K_R < 0$, $\xi(t)$ will approach the stable steady-state at $\xi_e$ (see Fig. 8). If $K_L < 0$ and $K_R > 0$, then $\xi(t)$ will move towards $x_R$ (see Fig. 9). Similarly, $\xi(t)$ will move towards $x_L$ if $K_L > 0$ and $K_R < 0$. When the spike touches $(x_L, 0)$ or $(x_R, 0)$, its subsequent evolution is determined by (2.19b).

# 6 Conclusion

We have given a quantitative characterization of the motion of a spike on the smooth boundary of a domain for the shadow problem (1.3). For a generic boundary, the spike moves towards a local maximum of the curvature in two dimensions and a local maximum of the mean curvature in three domains. In two dimensions, we have shown explicitly that

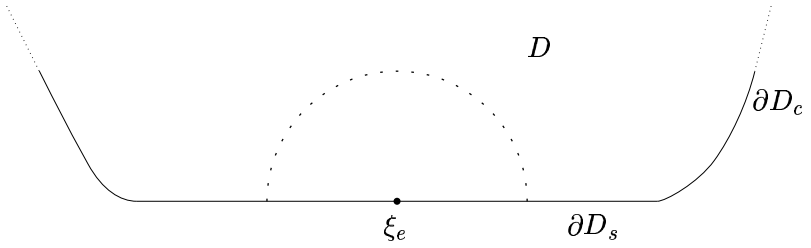


Figure 7: Plot of part of a domain boundary, $\partial D$, upon which the center of the spike is at an unstable steady state. $K_L > 0$, $K_R > 0$ for this domain.

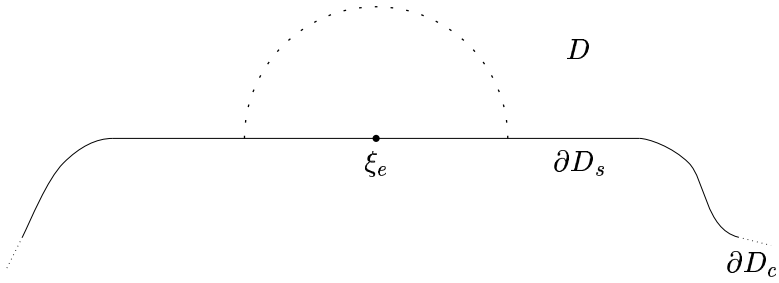


Figure 8: Plot of part of a domain boundary, $\partial D$, upon which the center of the spike is at a stable steady state. $K_L < 0$, $K_R < 0$ for this domain.

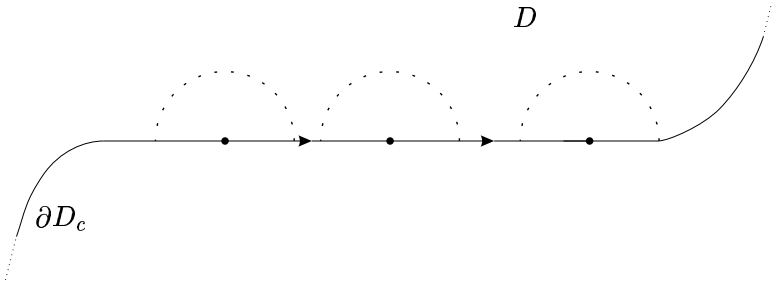


Figure 9: Plot of part of a domain boundary, $\partial D$, upon which the center of the spike moves towards the right. $K_L < 0$ and $K_R > 0$ for this domain.

the motion of a spike on a flat segment of the boundary is metastable. A similar result should hold in three dimensions. The critical feature that allows for the slow boundary spike motion is the presence of the nonlocal term in (1.3). This term eliminates a large unstable eigenvalue associated the local operator in (1.3). It would be interesting to determine the motion of a spike on the boundary for the full problem (1.1), which holds for finite inhibitor diffusivity, and to compare the results with those obtained above for the shadow problem. The problem of the existence of equilibrium boundary spikes for the full problem has been studied recently in [4].

## Acknowledgements

M. W. is grateful for the support of NSERC grant 81541. We would like to thank Prof. Andrew Bernoff for showing us the reference [16].

## A The Laplacian in the Boundary Layer Coordinate System

The derivation here is similar to that in [16]. We begin with a description of the boundary. Let $z = H(p_1, p_2)$ define the local height of the boundary at the point $(p_1, p_2)$ on the boundary. For convenience here we will center the coordinate system around the point $p_1 = 0$ and $p_2 = 0$, where $z = 0$. In terms of these coordinates, $H$ is given locally by

$$H(p_1, p_2) = \frac{1}{2}\kappa_1 p_1^2 + \frac{1}{2}\kappa_2 p_2^2 + O\left(p_1^2 + p_2^2\right) , \tag{A.1}$$

where $\kappa_1$ and $\kappa_2$ are the two principal curvatures at the center of the coordinate system. Our boundary layer coordinate system is $(p_1, p_2, \eta)$, where $\eta > 0$ is the distance from $\boldsymbol{x} \in D$ to $\partial D$. Therefore, we define the following change of coordinates,

$$\mathbf{x}(p_1, p_2, \eta) = (p_1, p_2, H(s_1, s_2)) + \eta\, \mathbf{n}(p_1, p_2) , \tag{A.2}$$

where $\mathbf{n}(p_1, p_2)$ is the unit normal to the boundary defined by,

$$\mathbf{n}(p_1, p_2) = \frac{(-H_{p_1}, -H_{p_2}, 1)}{\sqrt{1 + H_{p_1}^2 + H_{p_2}^2}}. \tag{A.3}$$

In order to find the Laplacian in these new coordinate, we must calculate the scale factors,

$$\nu_{p_1} = \left|\frac{\partial \mathbf{x}}{\partial p_1}\right| , \quad \nu_{p_2} = \left|\frac{\partial \mathbf{x}}{\partial p_2}\right| , \quad \nu_\eta = \left|\frac{\partial \mathbf{x}}{\partial \eta}\right| . \tag{A.4}$$

To evaluate these expressions, we substitute (A.1) and (A.3) into (A.2) and differentiate to find,

$$\nu_{p_1} = 1 - \eta\kappa_1 + O(p_1^2 + p_2^2 + \eta^2) , \tag{A.5a}$$

$$\nu_{p_2} = 1 - \eta\kappa_2 + O(p_1^2 + p_2^2 + \eta^2) , \tag{A.5b}$$

$$\nu_\eta = 1 . \tag{A.5c}$$

In general curvilinear coordinates, the Laplacian is given by,

$$\Delta\phi = \frac{1}{\nu_{p_1}\nu_{p_2}\nu_\eta}\left[\frac{\partial}{\partial p_1}\left(\frac{\nu_{p_2}\nu_\eta}{\nu_{p_1}}\frac{\partial\phi}{\partial p_1}\right) + \frac{\partial}{\partial p_2}\left(\frac{\nu_{p_1}v_\eta}{\nu_{p_2}}\frac{\partial\phi}{\partial p_2}\right) + \frac{\partial}{\partial\eta}\left(\frac{\nu_{p_2}\nu_{p_1}}{\nu_\eta}\frac{\partial\phi}{\partial\eta}\right)\right]. \tag{A.6}$$

Thus, in these variables, the Laplacian is given to within quadratic terms by

$$\begin{aligned}\Delta\phi = \phi_{\eta\eta} - \left(\frac{\kappa_1}{1-\eta\kappa_1} + \frac{\kappa_2}{1-\eta\kappa_2}\right)\phi_\eta + \frac{1}{(1-\eta\kappa_1)(1-\eta\kappa_2)}\partial_{p_1}\left(\frac{1-\eta\kappa_2}{1-\eta\kappa_1}\phi_{p_1}\right) + \\ \frac{1}{(1-\eta\kappa_1)(1-\eta\kappa_2)}\partial_{p_2}\left(\frac{1-\eta\kappa_1}{1-\eta\kappa_2}\phi_{p_2}\right) + O(p_1^2+p_2^2).\end{aligned} \tag{A.7}$$

This coordinate change is then used in (1.3a) to obtain (3.1).

# B An Asymptotic Estimation of an Inner Product

Now we bound the term $(\mathcal{L}_\epsilon^*[\partial_x u_c], \phi_1)$ in (5.20), where $\mathcal{L}_\epsilon^*$ is defined in (5.11). Since $\partial_x u_c$ satisfies the local part of the operator in (5.11), we obtain

$$\mathcal{L}_\epsilon^*[\partial_x u_c] = -\frac{mq\epsilon^{-2}u_c^{m-1}}{\beta\pi(s+1)}\int_D u_c^p\partial_x u_c\, d\mathbf{x}. \tag{B.1}$$

In §5 we assumed that the distance between $x=\xi$ and the curved part of the boundary $\partial D_c$ is minimized at one of the two corner points. Let $r_m = \min(x_R-\xi, \xi-x_L)$ denote this minimum distance. Let $B_r$ denote the semi-circle whose diameter is the interval $[\xi-r_m, \xi+r_m]$ along the $x$-axis. Then, by our assumption, $B_r$ must be strictly contained within $D$. We then decompose the integral in (B.1) as

$$\int_D u_c^p\partial_x u_c\, d\mathbf{x} = \int_{B_r} u_c^p\partial_x u_c\, d\mathbf{x} + \int_{D\setminus B_r} u_c^p\partial_x u_c\, d\mathbf{x}. \tag{B.2}$$

Since the point $x=\xi$, $y=0$ is the center of the semi-circle and the integrand is an odd function about the line $x=\xi$, the first integral on the right side of (B.2) is identically zero. Next, since $u_c$ decays exponentially away from the point $x=\xi$, $y=0$, the second integral on the right side of (B.2) is bounded by the maximum of the integrand on the boundary of $D\setminus B_r$ multiplied by the area $A_r$ of $D\setminus B_r$. In this way, using the far-field behavior (2.13b), we get

$$\left|\int_{D\setminus B_r} u_c^p\partial_x u_c\, d\mathbf{x}\right| \le C\epsilon^q e^{-(p+1)r_m/\epsilon}. \tag{B.3}$$

Here $q$ and $C$ are constants independent of $\epsilon$. Hence, in $D$, we have the estimate

$$|\mathcal{L}_\epsilon^*[\partial_x u_c]| \le C\epsilon^{q-2}u_c^{m-1}e^{-(p+1)r_m/\epsilon}, \tag{B.4}$$

for some new constant $C$. Since $\phi_1 \sim \partial_x u_c$, we can then use the same reasoning as described above to estimate $(\mathcal{L}_\epsilon^*[\partial_x u_c], \phi_1)$, where $\mathcal{L}_\epsilon^*[\partial_x u_c]$ is given in (B.4). We find

$$|\,(\mathcal{L}_\epsilon^*[\partial_x u_c], \phi_1)\,| \le C\epsilon^q e^{-(p+m+1)r_m/\epsilon}. \tag{B.5}$$

for some new constants $q$ and $C$ independent of $\epsilon$.

Finally, we compare (B.5) with the asymptotic order of the boundary integral in (5.20). The boundary integral in (5.20) is clearly $O\left(\epsilon^q e^{-2r_m/\epsilon}\right)$. However, since $p > 1$ and $m > 0$, it follows that the inner product term in (B.5) is asymptotically exponentially smaller than the boundary integral term in (5.20). Hence, we were justified in asymptotically neglecting the inner product term in (5.20).

## References


[1] N. Alikakos, X. Chen, G. Fusco, *Motion of a Drop by Surface Tension Along the Boundary*, (1998), preprint.

[2] U. Ascher, R. Christiansen, R. Russell, *Collocation Software for Boundary value ODE's,* Math. Comp., **33**, (1979), pp. 659-679.

[3] X. Chen, M. Kowalczyk, *Slow Dynamics of Interior Spikes in the Shadow Gierer-Meinhardt System*, Center for Nonlinear Analysis report No. 99-CNA-002, (1999), preprint.

[4] M. Del Pino, P. Felmer, M. Kowalczyk, *Boundary Spikes in the Gierer-Meinhardt System*, Center for Nonlinear Analysis report No. 99-CNA-003, (1999), preprint.

[5] A. Gierer, H. Meinhardt, *A Theory of Biological Pattern Formation*, Kybernetik, **12**, (1972), pp. 30-39.

[6] C. Gui, *Multi-peaked Solutions to a Semilinear Neumann Problem*, Duke Math. J., **84**, No.3, (1996), pp. 739-769.

[7] C. Gui, J. Wei, *Multiple Interior Peak Solutions for some Singularly Perturbed Neumann Problems*, J. Diff. Eq. (1999), to appear.

[8] L. Harrison, D. Holloway, *Order and Localization in Reaction-Diffusion Pattern*, Physica A, **222**, (1995) pp. 210-33.

[9] C. Hsiung, *A First Course in Differential Geometry*, Wiley Interscience Series in Pure and Applied Mathematics, Wiley, New York, (1981).

[10] D. Iron, M.J. Ward, *A Metastable Spike Solution for a NonLocal Reaction-Diffusion Model*, SIAM J. Appl. Math., (1999), to appear.

[11] M. Kowalczyk, *Multiple Spike Layers in the Shadow Gierer-Meinhardt System: Existence of Equilibria and Approximate Invariant Manifold*, to appear Duke Math J. (1999).

[12] M. Kowalczyk, *Exponentially Slow Dynamics and Interfaces Intersecting the Boundary*, J. Diff. Eq. **138**, No. 1, (1997), pp. 55-85.

[13] C. Lin, W. Ni, *On the Diffusion Coefficient of a Semilinear Neumann Problem*, in Calculus of Variations and Partial Differential Equations (Trento 1986), Lecture Notes in Math., 1340, Springer, Berlin-New York, (1988), pp. 160-174.

[14] W. Ni, *Diffusion, Cross-Diffusion, and their Spike-Layer Steady-States*, Notices of the AMS, Vol. **45**, No. 1, (1998), pp. 9-18.

[15] W. Ni, I. Takagi, *On the Shape of Least-Energy Solutions to a Semilinear Neumann Problem*, Comm. Pure Appl. Math, Vol. XLIV, (1991), pp. 819-851.

[16] D. Sarocka, A. Bernoff, *An Intrinsic Equation of Interfacial Motion for the Solidification of a Pure Hypercooled Melt*, Physica D, **85**, (1995), pp. 348-374.

[17] L. Shampine, M. Gordon, *Computer Solution of Ordinary Differential Equations, the Initial Value Problem*, W. H. Freeman publishers, San Fransisco (1975).

[18] A. Turing, *The Chemical Basis of Morphogenesis*, Phil. Trans. Roy. Soc. B, **327**, (1952), pp. 37-72.

[19] M. Ward, *An Asymptotic Analysis of Localized Solutions for Some Reaction-Diffusion Models in Multi-Dimensional Domains*, Stud. Appl. Math., **97**, No. 2, (1996), pp. 103-126.

[20] J. Wei, *On Single Interior Spike Solutions for the Gierer-Meinhardt System: Uniqueness and Stability Estimates*, Europ. J. Appl. Math., (1999), to appear.

[21] J. Wei, *Uniqueness and Eigenvalue Estimates of Boundary Spike Solutions*, (1998), preprint.

[22] E. Yanagida, *Stability of Stationary Solutions of the Gierer-Meinhardt System*, in China-Japan Symposium on Reaction-Diffusion Equations and their Applications and Computational Aspects (Shanghai 1994), World Sci. Publishing, River Edge, NJ (1997), pp. 191-198.